Band structure and Fermi surface of UPd_3 studied by soft x-ray angle-resolved photoemission spectroscopy

Ikuto Kawasaki,[1,*] Shin-ichi Fujimori,[1] Yukiharu Takeda,[1] Tetsuo Okane,[1] Akira Yasui,[1] Yuji Saitoh,[1] Hiroshi Yamagami,[1,2] Yoshinori Haga,[3] Etsuji Yamamoto,[3] and Yoshichika Ōnuki[3,4]

[1]*Condensed Matter Science Division, Japan Atomic Energy Agency, Sayo, Hyogo 679-5148, Japan*
[2]*Department of Physics, Faculty of Science, Kyoto Sangyo University, Kyoto 603-8555, Japan*
[3]*Advanced Science Research Center, Japan Atomic Energy Agency, Tokai, Ibaraki 319-1195, Japan*
[4]*Graduate School of Science, Osaka University, Toyonaka, Osaka 560-0043, Japan*

(Received 7 December 2012; published 26 February 2013)

Soft x-ray angle-resolved photoemission experiments have been performed to investigate the band structure and Fermi surface of UPd_3. We have observed three U $5f$ derived bands whose bandwidths are very narrow. Two of these bands appear around 0.8 eV and are slightly separated by about 0.2 eV. The presence of two bands at nearly the same energy might be due to the presence of the two inequivalent U sites. The other U $5f$ band appears around 1.8 eV. The energy separation between this band and the two nearly degenerate bands agrees with the $5f^1$-final-state multiplet model. In the vicinity of Fermi level, several highly dispersive bands, which form a holelike Fermi surface centered at the Γ point and an electronlike Fermi surface at the K point, were observed. These dispersive valence bands are qualitatively explained by a band structure calculation that assumes a localized $5f^2$ configuration. All these experimental observations are consistent with the localized U $5f$ nature.

DOI: 10.1103/PhysRevB.87.075142 PACS number(s): 79.60.−i, 71.18.+y, 71.20.−b

I. INTRODUCTION

Uranium-based compounds show various interesting properties, such as heavy fermion states, unconventional superconductivities, and multipole orderings. It is generally believed that these properties originate from the U $5f$ states. The $5f$ electrons have an intermediate character between localized $4f$ electrons of rare-earth compounds and itinerant $3d$ electrons of transition metals. To understand the nature of the U-based compounds, it is essential to clarify how the $5f$ electrons contribute to the formation of the band structure and Fermi surface (FS). In addition, it is also important to find an appropriate theoretical description for the $5f$ electronic states. Up to now, to address these issues, intensive experimental efforts have been devoted to various U-based compounds. Among various experimental methods, angle-resolved photoemission spectroscopy (ARPES) provides a direct probe of the band structure, and thus, it is a powerful method for studying the U $5f$ electronic states. Recently, ARPES experiments have been carried out for the itinerant uranium compounds UB_2 and $UFeGa_5$.[1,2] The U $5f$ derived energy band dispersion and FSs have been clearly observed in both the compounds, and it was found that the observed data are well explained by band-structure calculations based on local-density approximation (LDA).

In sharp contrast to these itinerant $5f$ compounds, UPd_3 is one of the most localized $5f$ uranium compounds. It crystallizes into a double hexagonal crystal structure where the two inequivalent U atoms occupy the pseudocubic and hexagonal positions.[3] Specific heat[4,5] and de Haas-van Alphen (dHvA) effect measurements[4–6] revealed that the effective mass of carriers is very small, indicating the absence of $5f$ states at Fermi level (E_F). Neutron scattering experiments observed crystalline electric field excitations of the $5f^2$ (U^{4+}) configuration and showed that the two inequivalent U sites have different crystalline electric field level schemes.[7] Moreover, various macroscopic and microscopic measurements revealed that the localized U $5f$ electrons exhibit four different phase transitions below 7.8 K, which are attributed to quadrupolar and magnetic orderings.[5,8–16] All these experimental observations are consistent with the localized $5f$ picture. Therefore, UPd_3 is an excellent example for studying the nearly localized U $5f$ states.

A number of photoemission experiments have been already carried out to study the U $5f$ electronic states in UPd_3. Angle-integrated photoemission (PES) and $5d$-$5f$ resonant PES studies revealed that the U $5f$ density of states (DOS) has a broad peak centered around 1 eV that spreads from 0.5 to 2.5 eV.[17–25] Ito *et al.* performed a detailed ARPES study using 21 eV photons.[26] Several highly dispersive bands in the vicinity of E_F and three nondispersive U $5f$ derived bands at 0.4 to 1 eV were observed. The observed nondispersive bands are consistent with the localized U $5f$ nature. However, the presence of the three nondispersive bands and the observed energy separation between each U $5f$ band are not consistent with the $5f^1$-final-state model.[27,28] Therefore, the origin of these U $5f$ bands was not clarified. In addition, the ARPES spectra cover a limited range of energy (E_F–1.2 eV) and do not cover the U $5f$ distribution observed by the PES studies.[17–25] Moreover, this ARPES experiment used low-energy photons and thus may have suffered from contamination of the surface electronic states. Therefore, further ARPES studies over a wide range of energy with enhanced bulk sensitivity are needed to clarify the U $5f$ electronic states.

In the present study, we have performed ARPES measurements for UPd_3 in the soft x-ray region (SX-ARPES) to clarify its electronic structure and to understand the nature of the U $5f$ state. SX-ARPES is a powerful experimental technique that probes the bulk electronic structure of strongly correlated electron materials.[1,2,29,30] We have successfully derived the three-dimensional band structure and FS of UPd_3. The obtained ARPES results are compared with a band

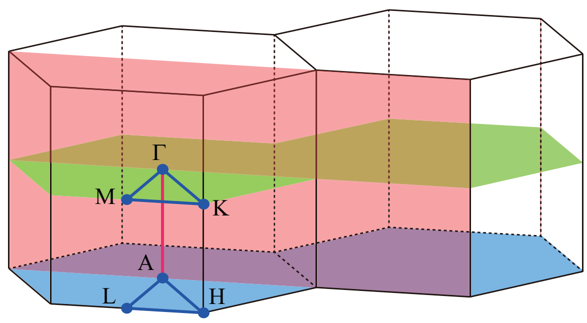

FIG. 1. (Color online) Brillouin zone of UPd_3 in the paramagnetic phase. The ARPES spectra in the green and blue planes were obtained by angle-scanning experiments while those in the red plane were obtained by $h\nu$-scanning experiments.

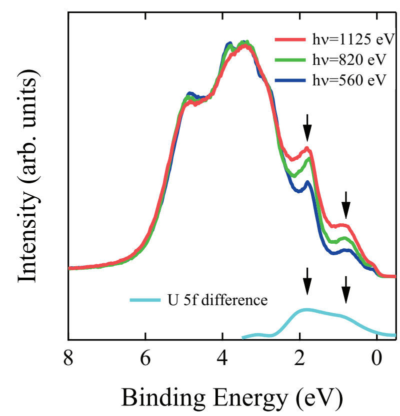

FIG. 2. (Color online) Angle-integrated spectra of UPd_3 in the paramagnetic phase measured with $h\nu = 560$, 820, and 1125 eV. These spectra were normalized to match the Pd 4d state. The U 5f spectrum was obtained by subtracting the 560 eV spectrum from the 1125 eV spectrum.

structure calculation, and the nature of the U 5f state in this compound is discussed.

II. EXPERIMENT

A UPd_3 single crystal was prepared by the Czochralski pulling method. SX-ARPES experiments were performed at SPring-8 BL23SU. A clean sample surface parallel to the (0001) plane was obtained by cleaving the sample *in situ* just before the measurements. During the experiments, the sample temperature was kept at 20 K, which is well above the quadrupolar and magnetic transition temperatures.[5,8–16] The base pressure was typically 2×10^{-10} mbar. The photoemission spectra were measured by a VG-SCIENTA SES2002 analyzer. The energy resolution was about 150 meV for the ARPES experiments with $h\nu = 770$–880 eV. The angular resolution along the analyzer slit was about $\pm0.22^\circ$, which corresponds to a $k_\parallel$ resolution of about 0.1 Å^{-1}. The momentum broadening along the $k_\perp$ direction due to the finite escape depth of photoelectrons (10–15 Å) was estimated to be about 0.06–0.1 Å^{-1}. These values are much smaller than the size of the Brillouin zone (BZ) of UPd_3 shown in Fig. 1, which is 1.46 Å^{-1} in the Γ-K direction and 0.65 Å^{-1} in the Γ-A direction.[3] In the present study, we changed the detection angle of photoelectrons and the incident photon energy in order to measure the three-dimensional band structure. The ARPES spectra in the Γ-M-K and A-L-H planes shown by the green and blue planes in Fig. 1 were obtained by changing the photoelectron detection angle at $h\nu = 820$ and 785 eV, respectively. In contrast, spectra in the perpendicular plane (indicated by the red plane) were obtained by the $h\nu$-scanning measurements from 770–880 eV. The position of E_F was referred to that of an evaporated gold film. To calculate the position of the ARPES scan in the BZ, we use a free electron final-state model with an inner potential value of $V_0 =$ 12 eV.[2] The band structure and FS of $ThPd_3$ were calculated using the relativistic linearized augmented plane-wave method within the LDA.[31] This band theory is based on the Dirac one electron equation, and thus, the spin-orbit interaction is naturally incorporated into the Hamiltonian without a second variational treatment. The obtained valence bands of $ThPd_3$ except for the 5f states correspond to those of UPd_3 with the localized U 5f^2 configuration, since the atomic number of Th atoms is two less than that of U atoms, though the 5f states in $ThPd_3$ are above E_F.

III. RESULTS AND DISCUSSION

Figure 2 shows the PES spectra of UPd_3 measured with $h\nu = 560$, 820, and 1125 eV at 20 K. In this energy range, the contributions of the U 5f and Pd 4d are dominant since they are more than one order of magnitude larger than those of other states such as Pd 5s, Pd 5p, and U 6d.[32] The observed spectra show many fine structures in the energy range from E_F to 6 eV, indicating the presence of many bands in this energy range. Relatively large DOS is observed from 2.5 to 6 eV, and this component hardly shows photon energy dependence. In contrast, the intensities of the two peaks designated by arrows at 0.8 and 1.8 eV increase with increasing the photon energy. According to a photoionization cross-section calculation, the relative photoionization cross section of U 5f states with respect to Pd 4d states enhances by a factor of about 1.5 upon increasing the photon energy from 560 to 1125 eV.[32] Therefore, we attribute the DOS in the binding energy range $E_B = 2.5$–6 eV mainly to Pd 4d states. This is consistent with the LDA calculation based on the localized 5f^2 configuration [to be shown in Fig. 3(b)], which predicts the presence of Pd 4d bands in this energy range. However, the peaks at 0.8 and 1.8 eV should have strong U 5f components. In order to extract the U 5f spectrum, we subtract the spectrum measured at 560 eV from that measured at 1125 eV. The difference spectrum, which represents the U 5f contribution and is shown at the bottom of Fig. 2, consists of two peaks as indicated by arrows. These peaks are at approximately 0.8 and 1.8 eV and correspond to the peaks of the PES spectra, although the peak at 1.8 eV is broader than the corresponding peak in the PES spectra. Note that although the intensities of these peaks in the U 5f spectrum are roughly comparable, the peak at 1.8 eV has a larger Pd 4d contribution. This is why the peak at 1.8 eV has a stronger intensity in the PES spectra. The U 5f DOS was investigated by the very recent 5d-5f resonance photoemission experiments where the observed 5f spectrum has very large width and is spreading from 0.5–2.5 eV in

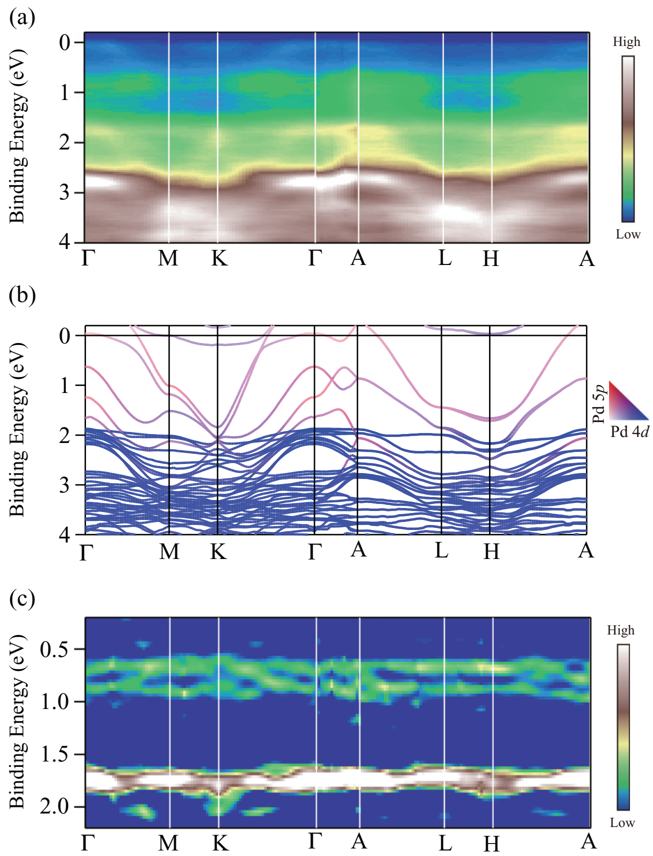

FIG. 3. (Color online) (a) ARPES spectral image of UPd_3 measured along the high-symmetry lines. (b) Calculated band structure of UPd_3. The colors of each band represent the contributions of Pd $5p$ and Pd $4d$ states. (c) Image plot of second derivatives of the ARPES spectra along the energy direction. The higher intensity part corresponds to the peak position in the energy distribution curves.

agreement with the present study.[24] Therefore, it was suggested that strong hybridization occurs between the U $5f$ and Pd $4d$ states. However, the present study clearly indicates that the primary cause of the large width of the U $5f$ spectrum is the presence of the two different peaks. Note that this scenario has already been proposed in early PES studies,[19,20] although they never clearly resolved the two peak structure.

Figure 3(a) shows an intensity plot of the ARPES spectra of UPd_3 along the several high-symmetry lines. These spectra are normalized to the area of each energy distribution curve. In the binding energy range deeper than 2.5 eV, dispersive bands with strong intensities were observed. These bands are expected to originate from Pd $4d$ states as shown in the PES spectra. In the vicinity of E_F, there are several dispersive bands, which appear to cross E_F; these bands are discussed in detail later. We observed less-dispersive spectral features at 0.8 and 1.8 eV. Based on the analysis of PES spectra, we suggest that the U $5f$ states contribute strongly to these spectral features.

Figure 3(b) shows the result of the LDA calculation for $ThPd_3$, which corresponds to the electronic state of UPd_3 in the localized $5f^2$ configuration. The band colors represent the contributions of Pd $5p$ and Pd $4d$ states. Below 2 eV, many dispersive bands exist with large contributions from the Pd $4d$ states. The calculation also predicts strongly dispersive bands in the energy range from E_F to 2 eV, and some of them cross E_F. According to the calculation, the primary component of these bands is the Pd $5p$ state, but the Pd $5s$ and U $6d$ states also contribute considerably to these bands. The calculated Pd $4d$ derived bands agree well with the experimentally measured bands in the binding energy range deeper than 2.5 eV. In addition, the less-dispersive spectral feature at 1.8 eV is also roughly reproduced by the calculation, since the weakly dispersive Pd $4d$ derived bands are predicted at a similar energy range. This is consistent with the fact that the spectral feature at 1.8 eV has a large Pd $4d$ contribution. However, we would like to stress that the PES results clearly indicate that this spectral feature also contains the U $5f$ component.

In order to see the details of the U $5f$ derived spectral features, we calculated the second derivatives of the ARPES spectra along with the energy direction to show the peak positions clearly. The resulting band structure is shown in Fig. 3(c). Less-dispersive bands at 0.8 and 1.8 eV were clearly observed. We found that the spectral feature at 0.8 eV consists of two different bands separated by about 0.2 eV. The dispersion of these bands is less than 0.1 eV, indicating that the U $5f$ electrons are nearly localized in this compound. The LDA calculation predicts several strongly dispersive bands in a similar energy range with the U $5f$ bands at 0.8 eV. However, we did not observe these bands. This may be because, as predicted by the calculation, these bands have large contributions from the Pd $5s$, Pd $5p$, and U $6d$ states whose intensities are quite weak in this photon energy range.[32] Although they were not observed experimentally, we expect that the hybridization between the U $5f$ bands and the highly dispersive bands predicted by the LDA is very weak, since the dispersion of the U $5f$ bands is very small. This also suggests that the U $5f$ state is absent around E_F and is consistent with the specific heat and dHvA studies.[4–6]

Next, we compare the present results with the previous ARPES study of Ito *et al.*[26] They reported three less-dispersive U $5f$ derived bands in the energy range of 0.4–1 eV. Two of them, located around 0.8 eV, agree well with the U $5f$ bands observed in this study. However, the other less-dispersive band located around 0.4 eV reported by Ito *et al.*[26] is absent from our spectra. The fact that the escape depth of the photoelectrons of the present SX-ARPES study (10–15 Å) is larger than that of the previous study, which used low-energy photons, suggests that the band reported at 0.4 eV might be a surface-derived band.

The origin of the two U $5f$ bands around 0.8 eV with slightly different energies is likely due to the presence of two inequivalent U sites that have different symmetry and thus should have different energy levels.[3] In fact, the neutron scattering experiments revealed that these U sites have different crystalline electric field level schemes.[7] In addition, the LDA + U calculation predicts that these U sites have slightly different electronic states.[33] The less-dispersive band at 1.8 eV might be understood as the other half of the $5f^1$-final-state multiplet, which is composed of two spin-orbit components $^2F_{5/2}$ and $^2F_{7/2}$. This is because the energy position of $^2F_{7/2}$ state is 0.9 eV deeper than that of $^2F_{5/2}$ state,[27] and the observed energy separation between the U $5f$ band at 1.8 eV and those located around 0.8 eV is very close to this energy difference. Note that the expected splitting of the U $5f$ band at

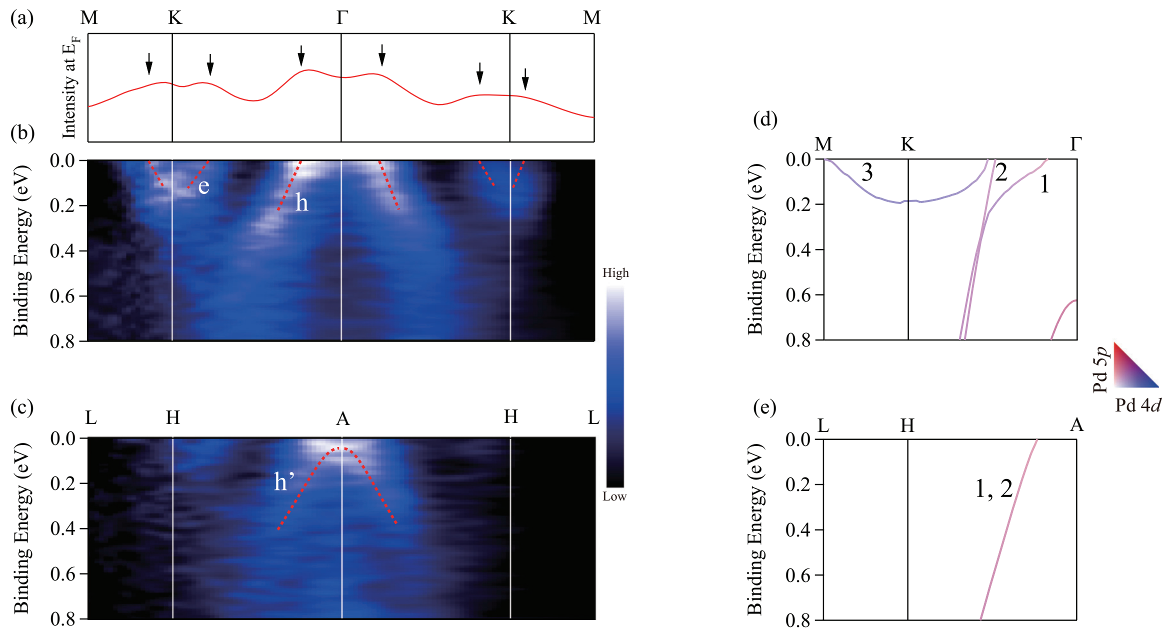

FIG. 4. (Color online) (a) Photoemission intensity at E_F measured along the Γ-K-M line. The arrows represent the estimated k_F. ARPES spectra normalized with the integrated intensities of the momentum distribution curves in the vicinity of E_F along (b) the Γ-K-M line and (c) the A-H-L lines. Broken red lines are guides to the eyes. Calculated band structures along (d) the Γ-K-M line and (e) the A-H-L line.

1.8 eV due to the presence of the two U sites was not observed. This might be due to the lifetime broadening effect. However, there is a large mismatch between the observed intensity ratio and that predicted by the $5f^1$-final-state multiplet model. The U $5f$ band at 1.8 eV and the bands at 0.8 eV have similar intensities in the difference spectrum in Fig. 2, whereas the predicted intensity ratio of between the $^2F_{5/2}$ and $^2F_{7/2}$ final states is 6 : 1 in the L-S limit. Moreover, upon approaching the j-j limit, the intensity of the $^2F_{7/2}$ final state should decrease further.[28] The reason for this large discrepancy is not clear at present, and therefore, the $5f^1$-final-state multiplet model cannot be simply applied to this system.

We now discuss the electronic structure in the vicinity of E_F. Figure 4(b) shows the band structure of UPd_3 near E_F along the Γ-K-M line. Here, we normalized the ARPES spectra so that the area of each momentum distribution curve should be unity. Since the Fermi-Dirac distribution function has the same value at a fixed energy, the Fermi-edge-cutoff effect is eliminated by this procedure. Bright points in this image correspond to peak positions in the momentum distribution curves. We found a holelike and an electronlike band across E_F, which are designated as h and e, respectively. Figure 4(a) shows the photoemission intensity at E_F; the peaks in this figure correspond to the positions of the Fermi momenta (k_F). Figure 4(c) shows the band structure along the A-H-L line. An inverted parabolic band with a maximum around 0.1 eV was observed, and we designate this band as h'. We also observed weak intensity around the H point in the left part of Fig. 4(c). Note that, as shown later, the band e forms a closed FS and does not exist at the H point. The weak intensity at the H point is most likely due to contamination of the intensity of the band e caused by the momentum broadening along the $k_\perp$, which is due to the finite escape depth of photoelectrons. Here, we note that the observed band structure is partially different from that of the previous study. For example, Ito *et al.*[26] also observed an electronlike band around the K point. The reported electronlike band has a bottom at 0.65 eV, whereas that of the band e is about 0.2 eV. Moreover, the presence of the additional holelike band, which has larger k_F than the band h and forms a large star-shaped FS, was reported. However, this band is absent in our spectra. This discrepancy might also be due to the different photoelectron escape depth.

To further understand these bands, we compare the experimentally obtained band structure with the results of the LDA calculation. Figures 4(d) and 4(e) show the calculated band structures along the Γ-K-M and A-H-L lines. We found that the calculation approximately reproduces the experimental band structure. For instance, along the Γ-K-M line, the electronlike band e corresponds to the calculated band 3, and the band h has a correspondence with the bands 1 and 2 of the calculation, which nearly overlap except around E_F. This suggests that the band h consists of two different bands, although we could not resolve the presence of two different bands. However, only one of these bands can cross E_F at the observed k_F and forms the FS. This is because, as discussed in later, the volumes of the observed holelike FS and electronlike FS are nearly the same in accord with the fact that this compound is a compensated metal, and thus, if the two bands cross E_F at the observed k_F, the compensation is violated. We speculate that the other band, which does not cross E_F at the observed k_F, has a maximum around E_F, and therefore, the observed intensity at E_F inside the k_F of the band h might be due to this band. For the A-H-L line, the band h' is well reproduced by the two degenerate bands 1 and 2 of the calculation, although the band h' does not cross E_F in contrast to the calculation. This comparison suggests that the band h' is identical to the band

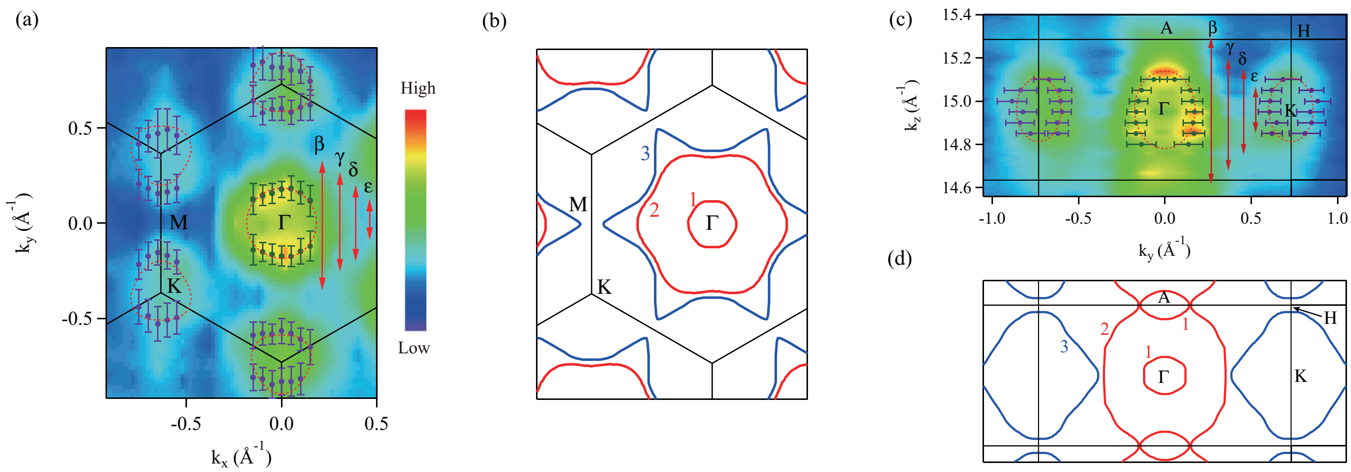

FIG. 5. (Color online) (a) FS image as a function of k_x and k_y at the Γ-M-K plane ($h\nu = 820$ eV). (c) FS image as a function of k_y and k_z obtained by $h\nu$-scanning measurements. The photoemission intensity is integrated over $E_F \pm 50$ meV. The k_F estimated from the band structure are indicated by solid green and purple symbols. The red arrows represent the size of the FSs reported by the dHvA experiments. (b), (d) Calculated FSs to be compared with the experiment. In (b) and (d), the red and blue lines represent the holelike and electronlike FSs, respectively.

h. The agreement between the experimental band structure and that of the LDA calculation for $ThPd_3$ provides further evidence that the localized U $5f^2$ configuration is plausible for this system.

In order to observe the FSs of UPd_3, we have made a two-dimensional image of the photoemission intensity integrated over $E_F \pm 50$ meV. Figure 5(a) shows the FS image obtained in the Γ-M-K plane ($h\nu = 820$ eV). Strong spectral intensities appear around the Γ and K points, suggesting the presence of FSs in these regions. To determine the detailed shape of the FSs, we superimpose the positions of k_F estimated from the band structure. The estimated k_F are shown as solid green and purple symbols. We found that the E_F crossing band h forms a closed holelike FS at the Γ point, and a closed electronlike FS derived from the band e centered at the K point was also observed. Figure 5(c) shows a two-dimensional image of the integrated photoemission intensity obtained from the $h\nu$-scanning measurements. The holelike FS derived from the band h centered at the Γ point and the electronlike FS derived from the band e centered at the K point were observed. From these FS slices, we estimate the volumes of the holelike and electronlike FSs to be about 0.025 and 0.014 $Å^{-3}$, and thus, the volume of the holelike FS is approximately twice that of the electronlike FS. Since the electronlike FS consists of two closed FSs, this indicates that compensation between the electronlike and holelike FSs is satisfied and is consistent with the fact that the unit cell of UPd_3 contains an even number of electrons.

For comparison, the calculated FSs are shown in Figs. 5(b) and 5(d). In the LDA calculation, the bands 1 and 2 form a small closed and a large open holelike FS, and the band 3 forms a multiply-connected electronlike FS along the K-K axis. According to the preceding discussion, the experimental FSs of the bands h and e correspond to the calculated FSs of the bands 2 and 3. In addition, the small holelike FSs originated from the band 1 seem to be absent in the ARPES spectra. Although the calculated FSs of the bands 2 and 3 are substantially larger than the experimental FSs, the basic structure of the experimental FSs still seems to be explained by the calculation. This is because if the calculated FSs of the bands 2 and 3 become slightly smaller, they will change into disconnected closed FSs with the same topology as the experimental FSs.

Finally, we compare the FSs obtained by the present ARPES study with those of the dHvA measurements.[5] The dHvA measurements reported several closed FSs β, γ, δ, and ϵ, which depend weakly on angle. By assuming a spherical shape for the FSs, the k_F values of these FSs are estimated to be about 0.34, 0.26, 0.20, and 0.11 $Å^{-1}$; the sizes of these FSs are shown by the red arrows in Figs. 5(a) and 5(c). The sizes of the holelike and electronlike FSs observed in the present study roughly correspond, within experimental uncertainties, to the dHvA branches γ and δ. However, this assignment is unlikely since the presence of a large undetected FS, which corresponds to the branch β, clearly breaks the electron-hole compensation regardless of whether the undetected FS is electronlike or holelike. Therefore, the FSs observed in the present study are not consistent with the dHvA results. Note that the dHvA experiments were performed at the low-temperature ordered phase,[5] and therefore, the discrepancy between the ARPES and dHvA results might originate in the change of the electronic structure arising from the quadrupolar and antiferromagnetic ordering.

IV. CONCLUSION

We have carried out bulk sensitive SX-ARPES measurements on UPd_3 and determined its three-dimensional band structure as well as its FSs. All of the observed U $5f$ bands show the less-dispersive feature, indicating a localized U $5f$ nature. Two U $5f$ bands, separated by about 0.2 eV, appear around 0.8 eV; the small separation in energy is likely explained by the presence of the two inequivalent U sites. The additional U $5f$ derived band appears at 1.8 eV. Its energy position is consistent with the prediction of the $5f^1$-final-state multiplet model; however, the observed intensity is not simply explained by the $5f^1$-final-state multiplet model, and thus, the origin of this band remains unclear. In the vicinity of E_F, we have observed several strongly dispersive bands that form a holelike FS centered at the Γ point and an electronlike FS at the K point, and it was found that these bands are qualitatively reproduced by a LDA calculation assuming a localized $5f^2$ configuration.

ACKNOWLEDGMENTS

This work was performed under Proposal No. 2011A3821 at SPring-8 BL23SU and was financially supported by Grants-in-Aid for Scientific Research on Innovative Areas Heavy Electrons (Grants No. 20102002 and No. 20102003) and a Grant-in-Aid for Scientific Research (S) (Grant No. 20224015) from the Ministry of Education, Culture, Sports, Science and Technology, Japan.

[*]Present address: Advanced Meson Science Laboratory, RIKEN Nishina Center for Accelerator Based Science, RIKEN, Wako, Saitama 351-0198, Japan; kawasaki_ikuto@riken.jp.

[1]T. Ohkochi, S. I. Fujimori, H. Yamagami, T. Okane, Y. Saitoh, A. Fujimori, Y. Haga, E. Yamamoto, and Y. Ōnuki, Phys. Rev. B **78**, 165110 (2008).

[2]S. I. Fujimori, K. Terai, Y. Takeda, T. Okane, Y. Saitoh, Y. Muramatsu, A. Fujimori, H. Yamagami, Y. Tokiwa, S. Ikeda, T. D. Matsuda, Y. Haga, E. Yamamoto, and Y. Ōnuki, Phys. Rev. B **73**, 125109 (2006).

[3]T. J. Heal and G. I. Williams, Acta Crystallogr. **8**, 494 (1955).

[4]S. W. Yun, H. Sugawara, J. Itoh, M. Takashita, T. Ebihara, N. Kimura, P. Svoboda, R. Settai, Y. Ōnuki, and H. Sato, J. Phys. Soc. Jpn. **63**, 1518 (1994).

[5]Y. Tokiwa, K. Sugiyama, T. Takeuchi, M. Nakashima, R. Settai, Y. Inada, Y. Haga, E. Yamamoto, K. Kindo, H. Harima, and Y. Ōnuki, J. Phys. Soc. Jpn. **70**, 1731 (2001).

[6]W. Ubachs, A. P. J. van Deursen, A. R. de Vroomen, and A. J. Arko, Solid State Commun. **60**, 7 (1986).

[7]W. J. L. Buyers and T. M. Holden, in *Handbook on the Physics and Chemistry of the Actinides*, edited by A. J. Freeman and G. H. Lander, Vol. 2 (Elsevier Science, Amsterdam, 1985), p. 239.

[8]S. W. Zochowski, M. de Podesta, C. Lester, and K. A. McEwen, Physica B **206-207**, 489 (1995).

[9]H. C. Walker, K. A. McEwen, D. F. McMorrow, S. B. Wilkins, F. Wastin, E. Colineau, and D. Fort, Phys. Rev. Lett. **97**, 137203 (2006).

[10]K. A. McEwen, J.-G. Park, A. J. Gipson, and G. A. Gehring, J. Phys.: Condens. Matter **15**, S1923 (2003).

[11]S. W. Zochowski and K. A. McEwen, Physica B **199-200**, 416 (1994).

[12]N. Lingg, D. Maurer, V. Müller, and K. A. McEwen, Phys. Rev. B **60**, 8430 (1999).

[13]U. Steigenberger, K. A. McEwen, J. L. Martinez, and D. Fort, J. Magn. Magn. Mater. **108**, 163 (1992).

[14]K. A. McEwen, U. Steigenberger, K. N. Clausen, J. Kulda, J.-G. Park, and M. B. Walker, J. Magn. Magn. Mater. **177-181**, 37 (1998).

[15]D. F. McMorrow, K. A. McEwen, U. Steigenberger, H. M. Rønnow, and F. Yakhou, Phys. Rev. Lett. **87**, 057201 (2001).

[16]H. C. Walker, K. A. McEwen, M. D. Le, L. Paolasini, and D. Fort, J. Phys.: Condens. Matter **20**, 395221 (2008).

[17]Y. Baer, H. R. Ott, and K. Andres, Solid State Commun. **36**, 387 (1980).

[18]B. Reihl, N. Mårtensson, D. E. Eastman, A. J. Arko, and O. Vogt, Phys. Rev. B **26**, 1842 (1982).

[19]A. J. Arko, D. D. Koelling, B. D. Dunlap, A. W. Mitchell, C. Capasso, and M. del Giudice, J. Appl. Phys. **63**, 3680 (1988).

[20]A. J. Arko, D. D. Koelling, B. D. Dunlap, C. Capasso, and M. del Giudice, J. Less-Common Met. **148**, 133 (1989).

[21]J.-S. Kang, J. W. Allen, M. B. Maple, M. S. Torikachvili, W. P. Ellis, B. B. Pate, Z.-X. Shen, J. J. Yeh, and I. Lindau, Phys. Rev. B **39**, 13529 (1989).

[22]L. Z. Liu, J. W. Allen, C. L. Seaman, M. B. Maple, Y. Dalichaouch, J.-S. Kang, M. S. Torikachvili, and M. A. Lopez de la Torre, Phys. Rev. Lett. **68**, 1034 (1992).

[23]J. W. Allen, J. D. Denlinger, Y. X. Zhang, G.-H. Gweon, S.-H. Yang, S.-J. Oh, E.-J. Cho, W. P. Ellis, D. A. Gajewski, R. Chau, and M. B. Maple, Physica B **281-282**, 725 (2000).

[24]M. F. Beaux, T. Durakiewicz, L. Moreschini, M. Grioni, F. Offi, G. Monaco, G. Panaccione, J. J. Joyce, E. D. Bauer, J. L. Sarrao, M. T. Butterfield, and E. Guziewicz, J. Electron Spectrosc. Relat. Phenom. **184**, 517 (2011).

[25]S.-I. Fujimori, T. Ohkochi, I. Kawasaki, A. Yasui, Y. Takeda, T. Okane, Y. Saitoh, A. Fujimori, H. Yamagami, Y. Haga, E. Yamamoto, Y. Tokiwa, S. Ikeda, T. Sugai, H. Ohkuni, N. Kimura, and Y. Ōnuki, J. Phys. Soc. Jpn. **81**, 014703 (2012).

[26]T. Ito, H. Kumigashira, S. Souma, T. Takahashi, Y. Haga, Y. Tokiwa, and Y. Ōnuki, Phys. Rev. B **66**, 245110 (2002).

[27]V. Kaufman and L. J. Radziemski Jr., J. Opt. Soc. Am. A **66**, 599 (1976).

[28]N. Beatham, P. A. Cox, A. F. Orchard, and I. P. Grant, Chem. Phys. Lett. **63**, 69 (1979).

[29]Y. Takeda, T. Okane, T. Ohkochi, Y. Saitoh, H. Yamagami, A. Fujimori, and A. Ochiai, Phys. Rev. B **80**, 161101 (2009).

[30]A. Sekiyama, S. Kasai, M. Tsunekawa, Y. Ishida, M. Sing, A. Irizawa, A. Yamasaki, S. Imada, T. Muro, Y. Saitoh, Y. Ōnuki, T. Kimura, Y. Tokura, and S. Suga, Phys. Rev. B **70**, 060506 (2004).

[31]H. Yamagami, J. Phys. Soc. Jpn. **67**, 3176 (1998).

[32]J. J. Yeh and I. Lindau, At. Data Nucl. Data Tables **32**, 1 (1985).

[33]A. N. Yaresko, V. N. Antonov, and P. Fulde, Phys. Rev. B **67**, 155103 (2003).